Radar Cross Section Measurement Comparison of UAVs at C-band and V-band

Oday Bshara, Yuqiao Liu, and Kapil R. Dandekar

Electrical and Computer Engineering Department, Drexel University, Philadelphia, PA, 19104, USA Email: {ob67, yl636, krd26}@drexel.edu

Abstract—Unmanned aerial vehicles (UAVs) are being used for civil, industrial, and military purposes. However, UAVs can pose threats when they leave their restricted routes or when they fly without permission. The proliferation of UAVs along with their potential threats raise the need for the development of detection and tracking systems for flying UAVs in predefined flying zones. Characterizing the radar cross section (RCS) signature of UAVs is crucial for the development of such systems. This paper measures angular monostatic RCS using vector network analyzer (VNA) S parameters to characterize a UAV based on its electromagnetic backscattering for both cases of stationary and rotating propellers at different speeds. Measurements were performed in an anechoic chamber and in a lab environment at 5 GHz and 60 GHz center frequencies, respectively.

I. INTRODUCTION

Unmanned aerial vehicles (UAVs), known as drones, are increasingly prevalent in everyday life. Hobbyists and photographers have an affordable bird's eye view for their scenes. Moreover, UAVs are being tasked with civil, industrial, and military applications due to their low cost, high maneuverability, small size, low operating altitudes, and increasing flight duration. For example, UAVs are being deployed in disaster relief missions, environmental data collection, flying base stations, crime scene and accident photography, and many other applications [1], [2], [3].

Apart from the benefits that UAVs are capable of, UAVs can pose civil privacy and military threats especially if we consider the implications of precise remote control features along with longer flight durations. It is alarming when you count the threats of an undetectable flying UAV that can be potentially utilized by malicious entities to monitor restricted or private properties, carry and drop dangerous materials, or smuggle illicit materials across borders [4]. Consequently, UAVs have to apply their geo-fencing feature to limit their flight only to specific zones for their particular purposes [2]. These geographic restrictions raise surveillance challenges since decisions and actions need to be taken rapidly if a UAV flies without permission or when it leaves its route. Detecting, identifying, and tracking UAVs through radar remote sensing, to enforce regulations and provide security, are ongoing research problems. Radars have been developed for detecting and tracking larger

flying objects like passenger airplanes. Unfortunately, radar systems can be limited when it comes to detecting objects with small radar cross section (RCS) such as UAVs flying at low altitudes where birds and background clutter decreases electromagnetic scattering signal to noise ratio (SNR) level and increases the missed detection probability as a result [5], [3]. The main contribution of this work is to provide radar cross section measurements for UAVs in reference to small objects of known RCS for both cases of stationary and rotating propellers at different speeds. RCS measurements were taken at 5 GHz and 60 GHz center frequencies and spanned 2 GHz. RCS signatures of UAVs are an intrinsic part of the development process of UAV detection and tracking systems. Our findings in this paper suggest a hybrid radar system that utilizes sub-6 GHz frequency RCS for detection, and mmWave frequency with wider bandwidth for identification through micro-Doppler signature classification.

The remaining parts of this paper are organized as below: section II surveys recent related work, section III shows our anechoic chamber and lab measurement setups, section IV details our measurements and main findings in this work, section V concludes our work.



Fig. 1: Anechoic chamber measurement setup. 4-6 GHz standard horn antenna of 20 dB nominal gain and 19° HPBW for both E and H planes. Object under test was supported by foam. UAV has been rotated in the azimuth direction as described in Figure 3.

II. RELATED WORK

The work in [6] performed anechoic chamber RCS measurements for reference objects and for random objects using a VNA. Specifically, they aimed to compare measurements of RCS in different facilities. The work in [7] contains similar work to ours at low frequencies. However, the measurement results appear noisy and were taken very close to their reference object. Unlike our paper, they have not applied background clutter removal techniques. The work in [5] addresses spurious background and clutter backscattering in RCS measurements, and is also relevant to our work. It described the importance of a background subtraction technique where an empty test zone is measured and subtracted from the measurements of loaded environment with the device under test (DUT). We used a similar method for suppressing background effects in our measurements.

The work in [8] showed the importance of exploring the unlicensed ISM mmWave bands including the 60 GHz band for radar systems to benefit from the available bandwidth to achieve higher resolution which is crucial in the detection of multiple UAVs. The work in [9] showed the advantage of higher frequencies in detecting the micro-Doppler modulation. The work in [10] ran experiments at 94 GHz that showed the feasibility of using mmWave frequencies for UAV detection and tracking. The work in [11] surveyed possible solutions for tracking and detecting UAVs including the use of mmWave frequencies. These papers emphasized the benefit of wider bandwidth for achieving higher resolution or the use of mmWave frequencies for detecting micro-Doppler signatures for UAV identification. We expand upon this idea in this paper to develop a testbed that is capable of jointly considering drone RCS (at lower frequencies) for detection and micro-doppler signatures (at mmWave frequencies) for identification. Micro-doppler measurements will be studied separately in our future work.

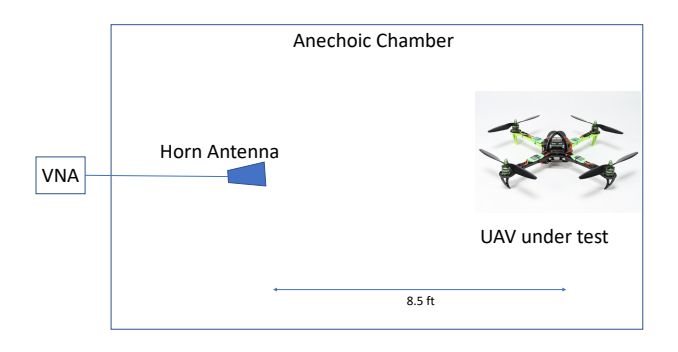


Fig. 2: Block diagram of the anechoic chamber measurement setup.



Fig. 3: UAVs used for collecting measurements. (Left) shows a DJI F550 Hexacopter , UAV $_1$ for short, and (Right) is a Turnigy SK450 Quadcopter powered by Multistar, UAV $_2$ for short. Top view is the one facing the horn antenna and is noted as 0° in the measurements section IV where it was then azimuthly rotated one complete cycle in 45° increments.



Fig. 4: RCS mmWave measurement setup. 1: KEYSIGHT 67 GHz PNA-X Network Analyzer N5247A, 2: 25 dBi standard horn antenna, 3: UAV₂ of Figure 3, 4: Fixed tripod, 5: Adjustable camera tripod.

III. MEASUREMENT SETUP

In the absence of a radar system, VNA measurements can be used to estimate RCS by measuring the backscattering along with the application of time domain gating [12]. In our sub-6GHz setup, one port of the VNA was attached to a standard horn antenna that works in the 4 - 6 GHz band. The port power was set to 10 dBm, the number of points was 16001, and a sweep time of 169 msec was used. The measurements took place in the anechoic chamber of Drexel Wireless Systems Laboratory. The UAV was supported by foam and placed at a distance of 8.5 ft from the horn antenna. Figure 1 shows our setup and

Figure 2 shows a block diagram of the same setup. In our 60 GHz measurement experiments we used our Keysight network analyzer that operates up to a frequency of 67 GHz. The measurement took place in a lab environment setup which is justified because of the pseudo line of sight propagation and significant attenuation of the signal at mmWave frequencies. We used a standard horn antenna of 25 dBi gain, and a diagram of our experimental setup is shown in Figure 4.

Calibration of the system to suppress systematic errors was done in three stages. First, VNA calibration was performed for the measurement range of 4 - 6 GHz and 59 - 61 GHz in order to take out the effect of the cable connection to the antenna. Second, we applied time gating at the VNA to suppress the effect of the antenna and other radiation sources apart from the UAV at low frequencies and applied time gating in post processing for the 60 GHz measurements as the VNA we used at high frequencies does not have the time domain option [13]. We will explain the time gating technique more in section IV. We used flat copper plates to identify the time gating center of the object of interest which was simply accomplished by tracking the time domain peaks of S11 without applying the time gating as we load the anechoic chamber with a flat copper plate. Third, S11 parameters were collected for the empty anechoic chamber and for the background clutter in the lab to suppress the background effect by subtracting empty chamber and unloaded lab environment measurements from the measurements of the DUT measurements.

IV. MEASUREMENTS AND RESULTS

RCS measurements are described in reference to an object with a known RCS. Two flat copper plates were used: one as a reference and the other for validation. We calibrated the measurement values by shifting them to be close to the calculated RCS of the reference plate according to the formula below [14]:

$$\sigma = \frac{64\pi a^2 b^2}{\lambda^2},\tag{1}$$

where σ is the radar cross section for rectangular flat plate of height 2b and of width 2a. UAV measurements experienced the same shifting we did to match plates calculated and measured values. Calculated RCS for the reference plates is shown in Fig. 6 at 5 GHz center frequency, and in Figure 8 for 60 GHz center frequency.

We made sure to apply the band pass time-gating option of the VNA at 4-6 GHz in order to save only the RCS of the UAV. Time gating is simply a time domain window option that filters out the reflections from other objects in the anechoic chamber including the reflections from the antenna itself. Figure 5 shows time domain measurements with and without time gating to illustrate the role of time gating in removing the effect of other

object reflections. Frequency S11 measurements were collected while applying the time gating function. A time gating hamming window was applied in post processing for the 60 GHz measurements. Matlab post processing subtracted the background measurements from UAV/Plateloaded anechoic chamber/lab environment to suppress any noise incurred by the anechoic chamber or lab reflections. UAV measurements then were shifted the same way we corrected the copper plates measurements to match the reference plates' calculated values to result in the UAV RCS.

To address the effect of incident angle of the sensor [15], the UAV was rotated 360° in 45° increments. Measurements are shown in Figure 6. Both UAVs have similar RCS depending on the incident angle. The materials making up the UAV are not very reflective in general, resulting in less RCS compared to both of the reference flat copper plates.

One more aspect we have measured was the effect of the rotating propellers on the RCS measurements. We mounted the SK450 Quadcopter shown in Figure 3 on a tripod. We powered the UAV by a power supply. UAV propeller motor controls were connected to a 6 channel digital servo tester in order to control the speed of the propellers. The speed was set manually through the servo tester knobs. A tachometer counter with a laser pointing at the rotating propeller was used to measure the speed in rotations per minute (RPM) for every propeller. Figure 7 shows a modulation effect on the sensor signal where it compares the stationary case with two different speed cases. For each speed, several trials of the same setup were measured. At high rotation speed, the curves were smoother, which was related to the sweep time of the VNA measurements.

UAVs usually fly at low altitudes. This makes it possible to cover short range UAV scanning despite the high attenuation at mmWave frequencies [11]. mmWave RCS signatures shown in Figure 8 resembled low frequency RCS measurements of reference metal plates, but with much higher values as equation (1) suggests. However, because of the use of narrow beam horn antennas, it was difficult to detect the object since a slight misalignment of the reflection angle causes a significant drop in the measured RCS. Thus, this is a problem that needs to be considered while designing a radar system that can suffer long scanning delays because of narrow beam high gain antennas. Alternatively, an electrically steerable antenna array with practical scanning delays can be used instead of fixed or mechanically steerable horn antennas. This finding also raised the need for developing a hybrid system that uses low frequencies for detection and tracking while benefiting from mmWave frequencies wider bandwidth and high RCS for the classification and identification of detected UAVs.

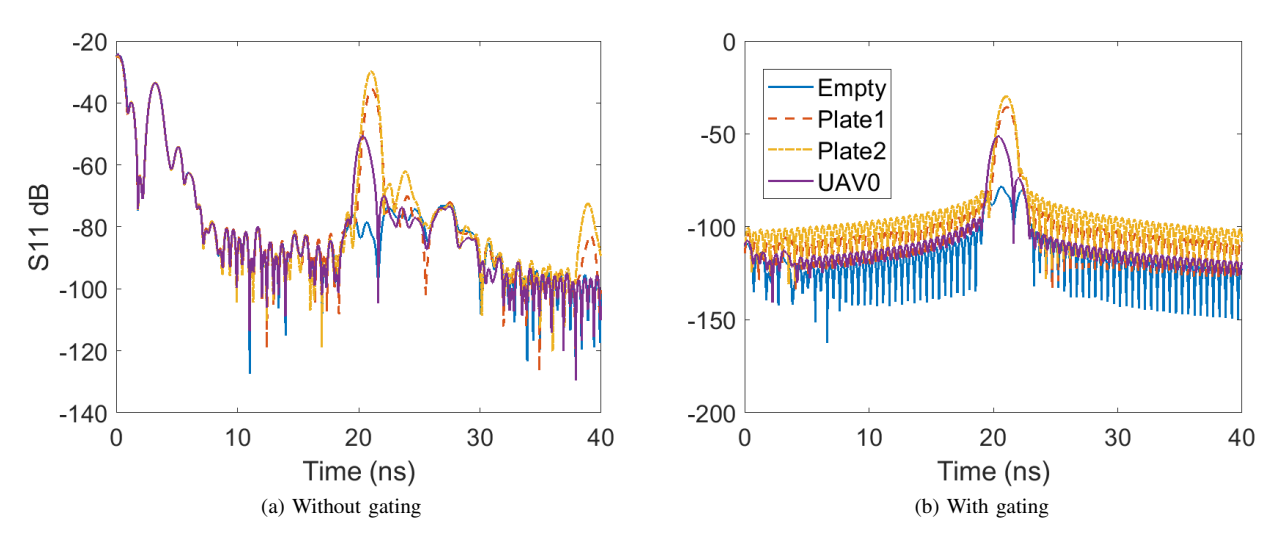


Fig. 5: Time domain RCS measurement. Band pass gating spanned 5 ns around the UAV back scattering peak.

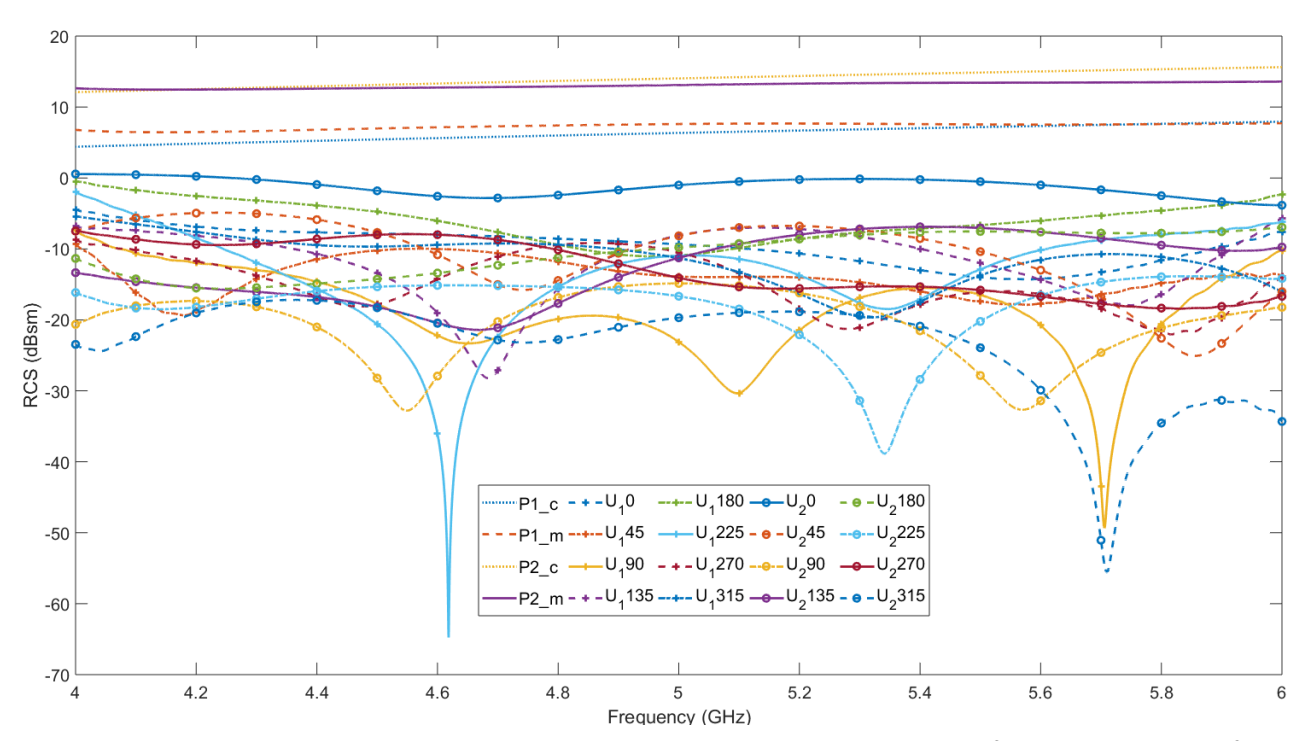


Fig. 6: RCS calculation and measurement for reference flat plates. Plate 1: $22.8 \times 15.4 cm^2$. Plate 2: $37 \times 23 cm^2$. RCS measurement for a complete cycle 45° increment rotations for the UAV. Legend: P \rightarrow Plate, $U_i \rightarrow UAV_i$, c \rightarrow calculated, m \rightarrow measurement.

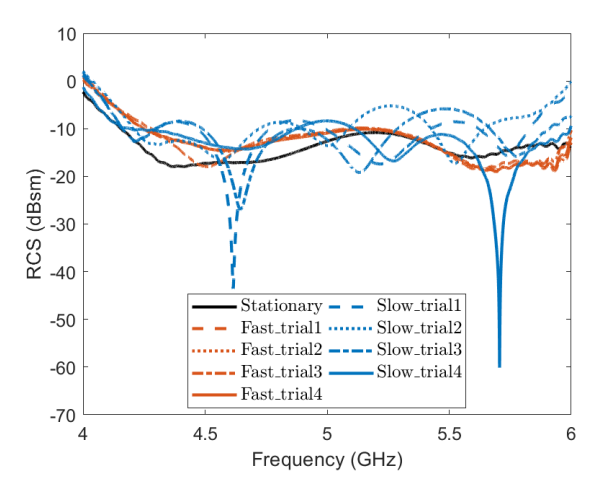


Fig. 7: RCS measurement while propellers are stationary or in rotation at low speed (1100 RPM) and high speed (2600 RPM).

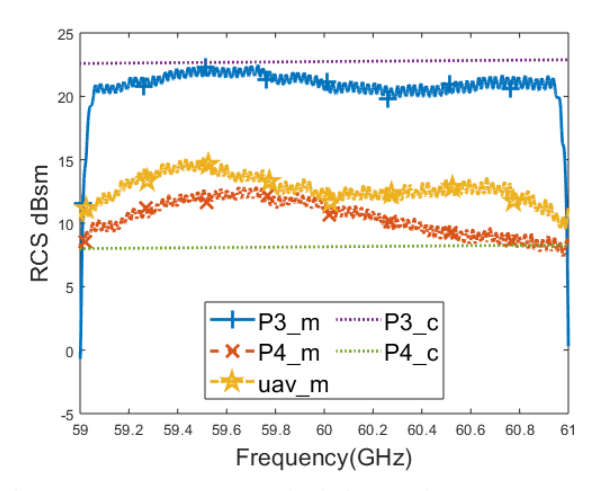


Fig. 8: mmWave RCS calculation and measurement for reference flat plates. Plate 3: $22.8 \times 15.4 cm^2$. Plate 4: $6 \times 6cm^2$. RCS measurement for a UAV $_2$ of Figure 3. Legend: P \rightarrow Plate, c \rightarrow calculated, m \rightarrow measurement.

They key takeaways of our measurements are as follows. First, UAV RCS is small compared to reference plates which calls for high power and high gain systems. Second, UAVs of different sizes and materials have different RCS signatures. This result can be used for the identification of UAVs. Third, the incident angle affects significantly the measured RCS especially at mmWave frequencies. These issues could be addressed by machine learning algorithms in the detection systems by including RCS measurements of different angles as training samples for each UAV or by benefiting from low frequency detection to align mmWave beams towards the detected UAVs. Finally, propeller speed affects the level of micro Doppler modulation in the RCS measurements and can

also be used in UAV identification.

V. CONCLUSION

Having access to measured RCS of UAVs will help design systems being developed for the sake of tracking UAVs and identifying adversarial UAVs in restricted zones. This paper described both an anechoic chamber and a lab environment setup for measuring RCS for different objects relative to a flat plate RCS at sub-6 GHz and mmWave frequencies. This work showed RCS measurements for a UAV at different incident wave angles. The results quantified RCS signatures at low and high frequencies for stationary and rotating rotors of UAVs. These signatures can be used for detecting a flying UAV. The significant deterioration of RCS levels at mmWave frequencies as a result of a misalignment between the antenna beam and the backscattering off the UAV motivates a hybrid system that utilizes mmWave for identification while relying on low frequencies for detection and tracking. Future work will combine micro-Doppler analysis with RCS signatures for precise identification of flying UAVs.

ACKNOWLEDGEMENT

This material is partially based upon work supported by the National Science Foundation under Grant No. CNS-1816387.

REFERENCES

- [1] M. Jacovic, O. Bshara, and K. R. Dandekar, "UAV Data Link Waveform Design Considerations for Interference in Urban Environments," in 2018 IEEE 85th Vehicular Technology Conference (VTC Fall), August 2018.
- [2] P. Blank, S. Kirrane, and S. Spiekermann, "Privacy-Aware Restricted Areas for Unmanned Aerial Systems," *IEEE Security Privacy*, vol. 16, no. 2, pp. 70–79, March 2018.
- [3] M. Jahangir and C. Baker, "Persistence surveillance of difficult to detect micro-drones with L-band 3-D holographic radar," in 2016 CIE International Conference on Radar (RADAR), Oct 2016, pp. 1–5.
- [4] X. Shi, C. Yang, W. Xie, C. Liang, Z. Shi, and J. Chen, "Anti-Drone System with Multiple Surveillance Technologies: Architecture, Implementation, and Challenges," *IEEE Communications Magazine*, vol. 56, no. 4, pp. 68–74, APRIL 2018.
- [5] L. To, A. Bati, and D. Hilliard, "Radar Cross Section measurements of small Unmanned Air Vehicle Systems in non-cooperative field environments," in 2009 3rd European Conference on Antennas and Propagation, March 2009, pp. 3637–3641.
- [6] F. Comblet, "Radar cross section measurements in an anechoic chamber: Description of an experimental system and post processing," in 2014 IEEE Conference on Antenna Measurements Applications (CAMA), Nov 2014, pp. 1–4.
- [7] C. C. Tsai, C. T. Chiang, and W. J. Liao, "Radar cross section measurement of unmanned aerial vehicles," in 2016 IEEE International Workshop on Electromagnetics: Applications and Student Innovation Competition (iWEM), May 2016, pp. 1–3.
- [8] M. Pauli, B. Gttel, S. Scherr, A. Bhutani, S. Ayhan, W. Winkler, and T. Zwick, "Miniaturized Millimeter-Wave Radar Sensor for High-Accuracy Applications," *IEEE Transactions on Microwave Theory and Techniques*, vol. 65, no. 5, pp. 1707–1715, May 2017.
- [9] V. C. Chen, F. Li, S. . Ho, and H. Wechsler, "Micro-Doppler effect in radar: phenomenon, model, and simulation study," *IEEE Transactions on Aerospace and Electronic Systems*, vol. 42, no. 1, pp. 2–21, Jan 2006.

- [10] M. Caris, W. Johannes, S. Stanko, and N. Pohl, "Millimeter wave radar for perimeter surveillance and detection of MAVs (Micro Aerial Vehicles)," in 2015 16th International Radar Symposium (IRS), June 2015, pp. 284–287.
- [11] I. Guven, O. Ozdemir, Y. Yapici, H. Mehrpouyan, and D. Matolak, "Detection, localization, and tracking of unauthorized UAS and Jammers," in 2017 IEEE/AIAA 36th Digital Avionics Systems Conference (DASC), Sept 2017, pp. 1–10.
- [12] R. D. P.-D. i Yague, A. B. Ibars, and L. F. Martinez, "Analysis and reduction of the distortions induced by time-domain filtering techniques in network analyzers," *IEEE Transactions on Instrumentation and Measurement*, vol. 47, no. 4, pp. 930–934, Aug 1998.
- [13] B. K. Chung, H. T. Chuah, and J. W. Bredow, "A microwave anechoic chamber for radar-cross section measurement," *IEEE Antennas and Propagation Magazine*, vol. 39, no. 3, pp. 21–26, Jun 1997.
- [14] R. Ross, "Radar cross section of rectangular flat plates as a function of aspect angle," *IEEE Transactions on Antennas and Propagation*, vol. 14, no. 3, pp. 329–335, May 1966.
- [15] H. Hatten, J. Seemann, J. Horstmann, and F. Ziemer, "Azimuthal dependence of the radar cross section and the spectral background noise of a nautical radar at grazing incidence," in *Geoscience and Remote Sensing Symposium Proceedings*, 1998. IGARSS '98. 1998 IEEE International, vol. 5, Jul 1998, pp. 2490–2492 vol.5.